Available online at www.sciencedirect.com

ScienceDirect

Journal of Magnesium and Alloys 1 (2013) 275–282
www.elsevier.com/journals/journal-of-magnesium-and-alloys/2213-9567

Full length article

Dependence of flow strength and deformation mechanisms in common wrought and die cast magnesium alloys on orientation, strain rate and temperature

S. Xu [a,*], W.R. Tyson [a], R. Eagleson [a], R. Zavadil [a], Z. Liu [b], P.-L. Mao [b], C.-Y. Wang [b], S.I. Hill [c], A.A. Luo [d]

[a] *CanmetMATERIALS, Natural Resources Canada, 183 Longwood Road South, Hamilton, ON L8P 0A1, Canada*
[b] *School of Material Science and Engineering, Shenyang University of Technology, 111 Shenliao West Road, Shenyang 110870, PR China*
[c] *University of Dayton Research Institute, 300 College Park, Dayton, OH 45469-0133, USA*
[d] *General Motors Research & Development Center, Warren, MI 48090, USA*

Received 12 October 2013; accepted 7 November 2013

Abstract

The controlling plastic deformation mechanisms (i.e. slip or twinning) and the structural crash performance of Mg alloys are strongly influenced by loading mode, texture and microstructure. This paper summarizes the main results from an experimental program to assess these effects for commercial Mg alloy extrusions (AM30 and AZ31), sheet (AZ31), and high pressure die castings (HPDC, AM50 and AM60). Uniaxial tensile and compressive tests were performed over a wide range of strain rate and temperature (i.e. 0.00075–2800 s^{-1} and 100 °C to −150 °C) using conventional servo-hydraulic and high-strain-rate universal test machines and a split-Hopkinson-bar (SHB) apparatus. In primarily-slip-dominant deformation, the true stress–strain curves showed approximate power-law behavior, and the effects of strain rate and temperature on yield strength could be approximately described by constitutive equations linearly dependent on the rate parameter, $T\ln(5.3 \times 10^7/\dot{\varepsilon})$ where T is test temperature in Kelvin and $\dot{\varepsilon}$ is strain rate in s^{-1}. In primarily-twin-dominant deformation, the effects of strain rate and temperature on yield and initial flow stress were negligible or small from quasi-static to 2800 s^{-1} owing to the athermal characteristics of mechanical twinning; the effects may become more pronounced with exhaustion of twinning and increasing proportion of slip.

Keywords: Constitutive equation; Effects of strain rate and temperature; Effects of orientation; Crashworthiness; Magnesium alloy

1. Introduction

Magnesium and its alloys have hexagonal close-packed (HCP) crystal structure and activation of several variants of both slip systems and twin systems is required for an arbitrary shape change. Dislocation slip in HCP crystals includes both basal and non-basal systems. For Mg and its alloys, the critical resolved shear stress (CRSS) of basal slip is less affected by strain rate and temperature than non-basal slip [1,2], especially for pure magnesium [2]. Deformation in *c*-axis tension may occur by tensile $\{10\bar{1}2\}$ twinning and in *c*-axis compression by double twinning e.g. Refs. [3,4]. The critical stress to activate tensile twinning is lower than that for compression twinning e.g. Refs.

* Corresponding author.
E-mail address: sxu@nrcan.gc.ca (S. Xu).
Peer review under responsibility of National Engineering Research Center for Magnesium Alloys of China, Chongqing University

Production and hosting by Elsevier

http://dx.doi.org/10.1016/j.jma.2013.11.003.

Table 1
Nominal compositions of Mg alloys used in this study.

Alloy	Mg	Al	Mn	Zn
AM30	Balance	3.0	0.4	–
AZ31	Balance	3.0	0.2	1.0
AM50	Balance	5.0	0.4	–
AM60	Balance	6.0	0.3	–

[5,6]. Experimental work has shown that plastic deformation of Mg alloys can be slip-dominant or twinning-dominant depending on loading, texture and microstructure e.g. Ref. [7]. The effects of strain rate and temperature on yield and flow stress, as well as the structural performance under crash conditions, are strongly influenced by the controlling deformation mechanisms and therefore by loading mode, texture and microstructure.

To quantitatively investigate these effects, an experimental program in a collaborative three-country project on Magnesium Front-End Research and Development (MFERD) [8] was undertaken for commercial Mg alloy extrusions (AM30 and AZ31), sheet (AZ31), and high pressure die castings (HPDC, AM50 and AM60) over a range of strain rate and temperature. The results form a database for crashworthiness design and simulation, material selection and development of constitutive equations.

2. Materials and procedures

2.1. Materials

Five commercial Mg–Al–Mn and Mg–Al–Zn alloys were used, including thick AM30 and AZ31 extrusions (section thickness 22 mm), 2-mm thick AZ31 sheet, and 3-mm thick AM50 and AM60 high-pressure die castings (HPDC). Details of chemical compositions, microstructures and textures of the AM30 and AZ31 extrusions are reported elsewhere [9–11]. For comparison, nominal compositions of AM30, AZ31, AM50 and AM60 are given in Table 1. The wrought Mg alloys had relatively uniform grain sizes as shown in Fig. 1a for AZ31 sheet while the HPDC alloys exhibited very fine grains near the die-skins (Fig. 1b) and grain sizes in the center of about 23–35 μm (Fig. 1c).

Wrought Mg alloys are usually textured owing to the predominance of basal slip during processing. Textures in the test sections of the extrusions were determined [9,11] and showed that the *c*-axis was parallel to the transverse direction (TD). The textures in the extrusions are schematically shown in Fig. 2a (note that ED in Fig. 2a refers to extrusion direction).

Textures of the AZ31 sheet and HPDC AM50 and AM60 alloys were not experimentally characterized in this work. However, it is known that Mg sheet has pronounced texture with the *c*-axis perpendicular to the rolling plane (Fig. 2b) e.g., Ref. [12] (Note that for sheet material RD refers to rolling direction and TD to transverse direction). HPDC Mg castings usually have random texture [13].

2.2. Specimens

For tests using a conventional servo-hydraulic test machine, extrusion tensile specimens were round tensile "dog bones" with a gauge length of 25.4 mm and diameter of 6.34 mm and compression specimens were cylinders 19.1 mm in height and 6.35 mm in diameter [9,11]. For the sheet and HPDC alloys

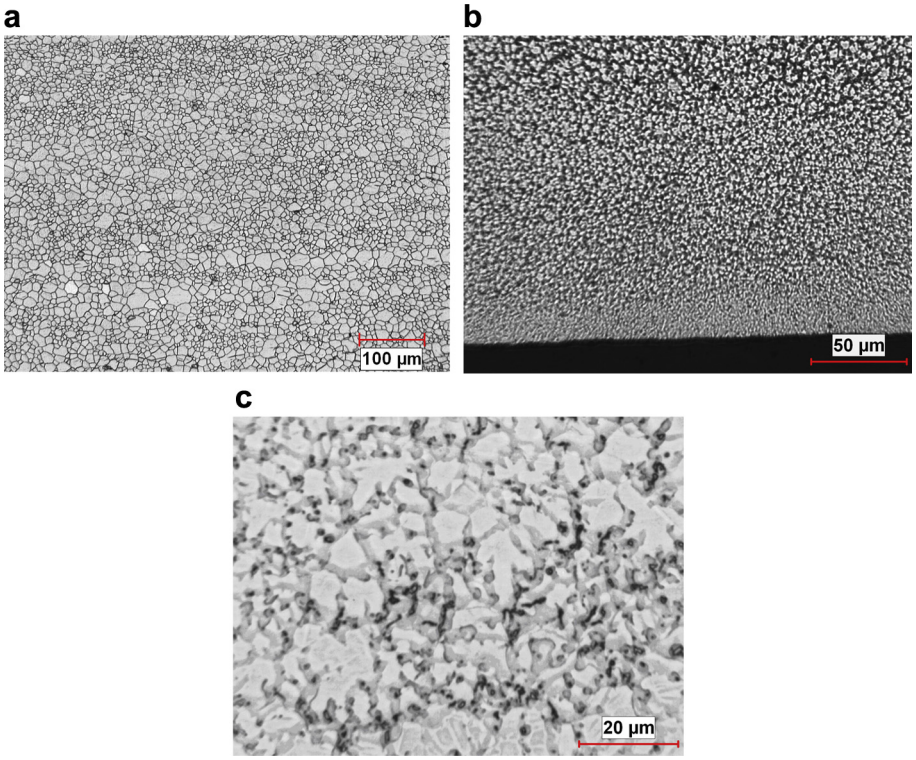

Fig. 1. Optical micrographs of sheet and HPDC alloys. (a) AZ31 sheet (rolling direction) (b) HPDC AM50 (skin region) (c) HPDC AM50 (center region).

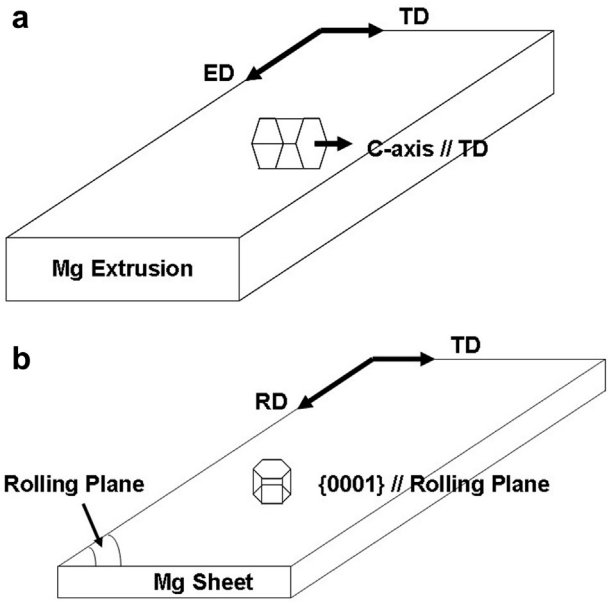

Fig. 2. Schematic of orientation and texture. (a) Extrusion (b) Sheet.

tensile specimens were full thickness with a gauge length of 25.4 mm.

For tests using a high-rate test machine, tensile specimens were flat "dog bones" per ASTM D 638 Type V, with a straight and parallel section of dimensions 3.18 mm (w) × 9.25 mm (l) × 2.4 mm (t). Compression specimens were flat rectangles with dimensions 9.52 mm (w) × 33.5 mm (l) × 2.4 mm (t) [8].

For tests using a split-Hopkinson bar (SHB) apparatus, extrusions tensile specimens had a gauge section of 8 mm and diameter of 4 mm. Sheet and HPDC alloys specimens were full thickness with a gauge length of 8 mm. Extrusions compressive specimens were cylindrical with length of 6 mm and diameter of 10 mm.

2.3. Testing

Uniaxial tests were performed using a conventional servo-hydraulic test machine and an environment chamber in well-controlled test conditions over a range of strain rate and temperature (i.e. 100 °C to −150 °C and 0.00075 to 9 s^{-1}) at CANMET-Materials Technology Laboratory (CANMET). Uniaxial tests were also carried out using a high-strain-rate test machine at room temperature and strain rate from 10 s^{-1} up to 800 s^{-1} at the University of Dayton Research Institute (UDRI). In addition, split-Hopkinson bar (SHB)

Table 2
Tensile and compressive properties of Mg alloys at a quasi-static rate and 22 °C.

Alloy/Process	Orientation	Loading	YS (MPa)	Elongation or strain to failure (%)[a]
AM30/extrusion	ED	Tensile	196	12.3
		Compressive	84	12.8
	TD	Tensile	76	19.1
		Compressive	119	8.3
AZ31/extrusion	ED	Tensile	213	12.4
		Compressive	104	10.8
	TD	Tensile	96	21.5
		Compressive	115	7.7
AZ31/sheet	RD	Tensile	156	27.6
	TD	Tensile	187	23.0
AM50/HPDC	–	Tensile	114	15.4
AM60/HPDC	–	Tensile	126	15.1

[a] Note that the gauge length is 25.4 mm for tensile and 19.1 mm for compressive specimens, respectively.

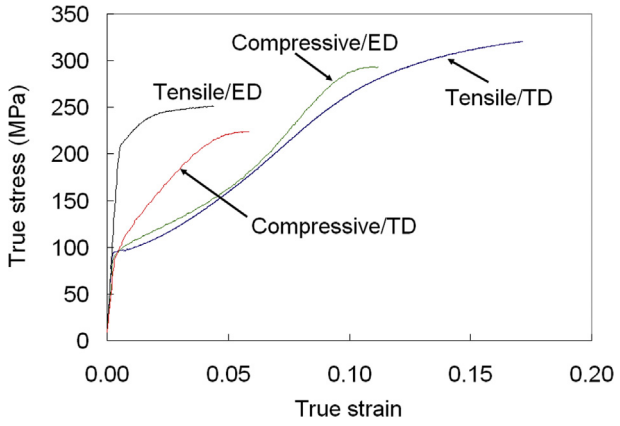

Fig. 3. Stress–strain curves of AZ31 extrusion tested at 23 °C and quasi-static rate.

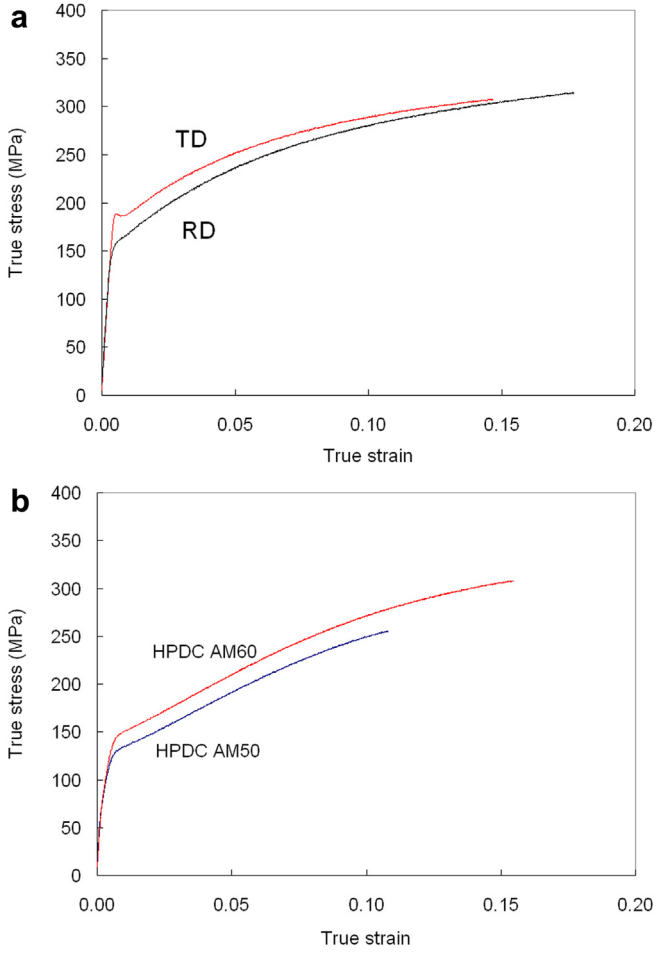

Fig. 4. Stress–strain curves of sheet and HPDC alloys. (a) AZ31 sheet (b) HPDC AM50 and AM60 alloys.

testing tasked to the Shenyang University of Technology (Shenyang) was employed to achieve even higher strain rates from 500 s^{-1} up to 2800 s^{-1} at room temperature.

3. Results and discussion

3.1. Orientation and loading effects and deformation mechanisms

Tensile and compressive properties at room temperature of the five Mg alloys are reported in Table 2.

The dependence of flow strength and deformation mechanisms on orientation and loading mode shown in Table 2 and Fig. 3 result from the textures and twinning asymmetry in the alloys and are reflected in the shape of stress–strain curves. In this work, these effects can be best illustrated in tensile and compressive tests of the extrusions in both ED and TD directions. Fig. 3 shows true stress–strain curves of the AZ31 extrusion; similar results were obtained in the AM30 extrusion [10]. Tensile deformation parallel to the basal planes was slip-dominant, such as for the extrusion specimens taken along the extrusion direction (ED) (see Fig. 3 and [9,11]). In slip-dominant deformation, the true stress–strain curves of Mg alloys showed approximately power-law behavior. Note that for tensile loading along the ED of the extrusions, stress is applied almost parallel to the basal plane, the stress on the basal plane is near zero and therefore, the slip is non-basal (i.e. prismatic or pyramidal slip); the stress levels are accordingly higher than for basal slip.

For the extrusions, for tensile TD and compressive ED tests (twinning-dominant deformation), stress increased with strain sigmoidally (Fig. 3). This is consistent with the known characteristics of the "basic" $\{10\bar{1}2\}$ twins producing tension strain. The compressive TD specimens exhibited flow curves

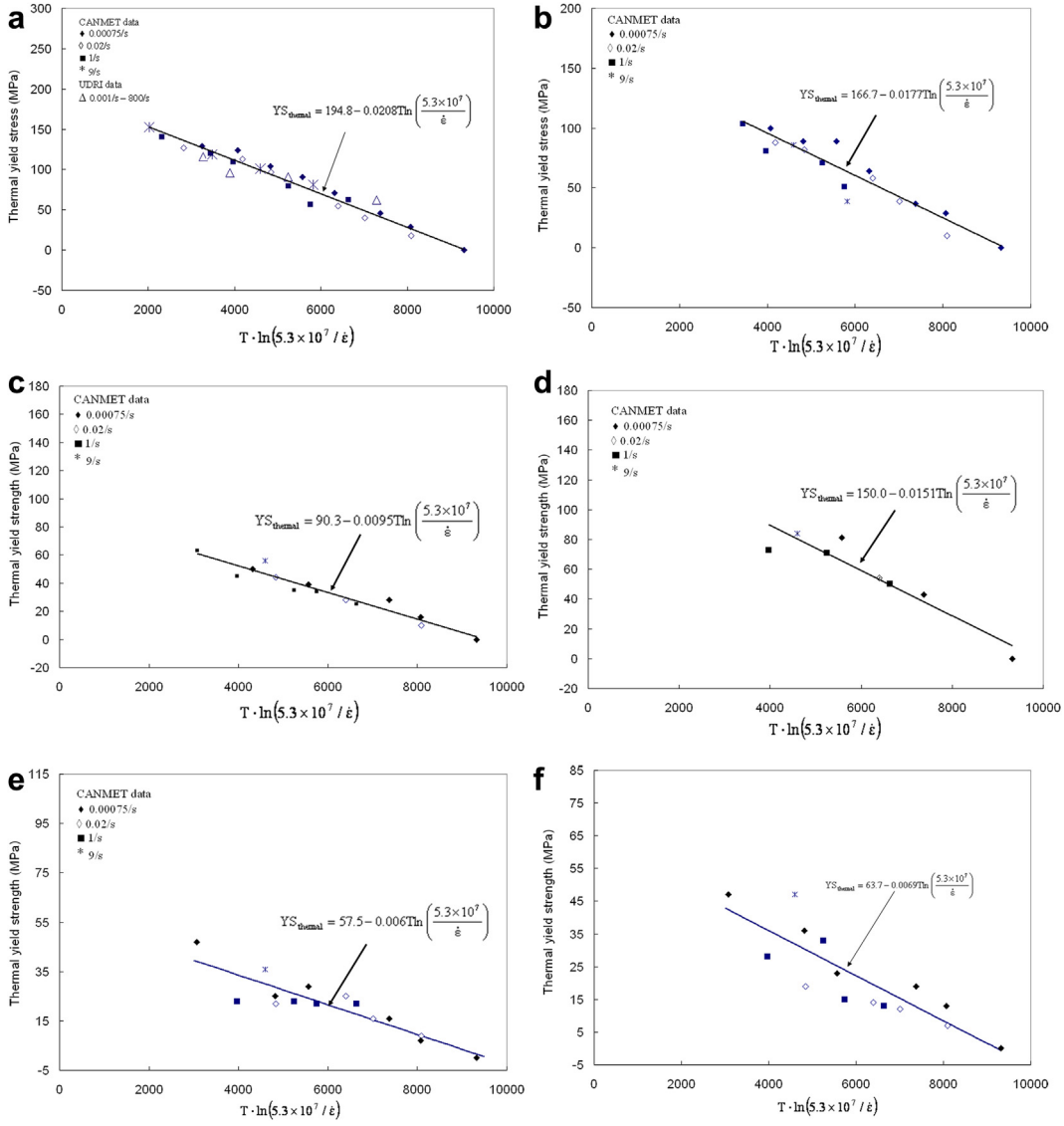

Fig. 5. Thermal yield strength vs. rate parameter of Mg alloys. (a) AM30 extrusion, tensile/ED (σ_{ath} = 150) (b) AZ31 extrusion, tensile/ED (σ_{ath} = 176) (c) AZ31 sheet, tensile/RD (σ_{ath} = 128) (d) AZ31 sheet, tensile/TD (σ_{ath} = 144) (e) HPDC AM50, tensile (σ_{ath} = 98) (f) HPDC AM60, tensile (σ_{ath} = 107).

typical of those controlled by a double-twinning mechanism and were intermediate to those of slip-dominant and tension-twin-controlled mechanisms.

For the sheet specimens loaded along the rolling direction (RD) and transverse direction (TD) (Fig. 4a), the stress–strain curves showed approximate power-law behavior and the deformation mechanism was slip-dominant. The texture is responsible for lower yield strengths in RD samples than in TD samples e.g., Ref. [12]. High pressure die castings usually have random textures and fine grains. The slip mechanism was important or dominant in the Mg die castings. The true stress–strain curves of HPDC AM50 and AM60 alloys, displayed in Fig. 4b, can also be approximated as power-law behavior.

3.2. Effects of strain rate and temperature

3.2.1. Dislocation-slip-dominant deformation

The rate-sensitive yield strength data from the conventional servo-hydraulic test machine were analyzed using dislocation thermal activation theory (twinning activity is considered to be athermal) e.g. Ref. [9] to derive empirical constitutive equations. In order to validate the constitutive equations, data at higher strain rates using the high-rate machine and the SHB apparatus related to crashworthiness applications were compared to the predictions from the constitutive equations.

For crashworthiness design and simulation, the whole stress–strain curve is needed. The flow strength of dislocation-dominant deformation of Mg alloys can be expressed as an athermal component (depending on strain and microstructure) and a thermal component (depending on strain rate and temperature) as

$$\sigma = \sigma_{\text{ath}} + \sigma_{\text{th}} = \sigma_{(\text{quasi-static},100\,^{\circ}\text{C})} + \sigma_{\text{th}} \quad (1)$$

The athermal stress can be taken as that measured at 100 °C and quasi-static rate and the thermal stress as a function of the rate parameter $T\ln(10^8/\dot{\varepsilon})$ which is determined from yield strength values measured over a range of strain rate and temperature.

For dislocation-slip-dominant deformation, the thermal yield strengths (i.e. measured yield strength minus the athermal yield strength σ_{ath} measured at quasi-static rate and 100 °C) as a function of the rate parameter are shown in Fig. 5. As the temperature decreases and/or strain rate increases, the rate parameter decreases and the thermal component of strength increases. The thermal yield strengths of the Mg alloys could be fitted linearly to the rate parameter; the equations in Fig. 5 represent best linear fits. The constitutive equations are given in Fig. 5 including the athermal yield strength values in figure captions. The apparent activation volume of the thermally activated process could be evaluated from the slope $\mathrm{d}(T\ln(\dot{\varepsilon}_0/\dot{\varepsilon}))/\mathrm{d}\sigma$ [9] and ranges from 11 to 38 $\mathbf{b}^3$ (where **b** is the Burgers vector for magnesium) for the Mg alloys.

The constitutive equation for tensile ED of the AM30 extrusion was compared with the tensile data using the high-rate test machine and displayed very good agreement.

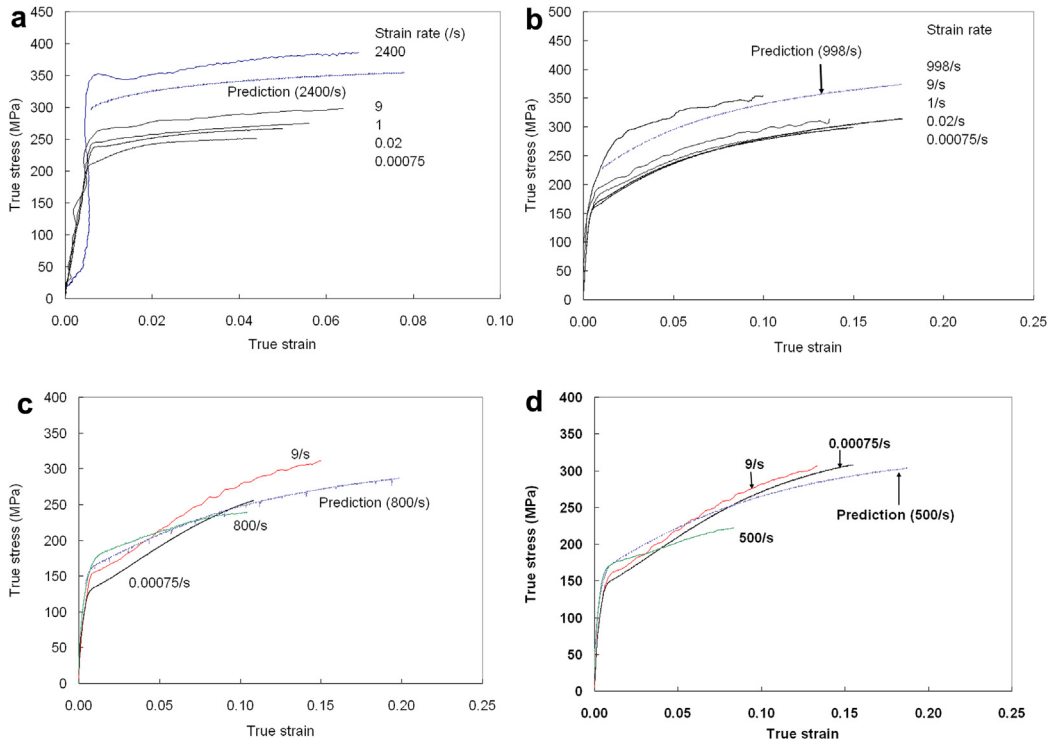

Fig. 6. Stress–strain curves using the conventional universal test machine, SHP and constitutive equations. (a) AZ31 extrusion, tensile/ED (b) AZ31 sheet, tensile/RD (c) HPDC AM50, tensile (d) HPDC AM60, tensile.

Table 3
Athermal and thermal yield strengths of wrought and die cast Mg alloys.

Alloy/process	Specimen orientation	Loading	σ_{ath} (MPa)	A (MPa), B (MPa/K) in $A - B\,T\ln\left(\frac{5.3\times10^{7}}{\dot{\varepsilon}}\right)$
AM30/extrusion	ED	Tensile	150	194.8, 0.0208
AZ31/extrusion	ED		176	166.7, 0.0177
AZ31/sheet	RD		128	90.3, 0.0095
	TD		144	150.0, 0.0151
AM50/HPDC	–		98	57.5, 0.006
AM60/HPDC	–		107	63.7, 0.0069

Stress–strain curves obtained using a conventional universal test machine (strain rate range 0.00075–9 s^{-1}), the SHB technique, and the prediction from the constitutive equations for high rates is shown in Fig. 6. It is well known that using the SHB technique the initial deformation stage is poorly resolved and accurate values of yield strength cannot be obtained. The prediction from the constitutive equations equals the athermal flow stress determined from the quasi-static rate testing at 100 °C plus the thermal stress as defined in the equations given in Table 3. It has been assumed

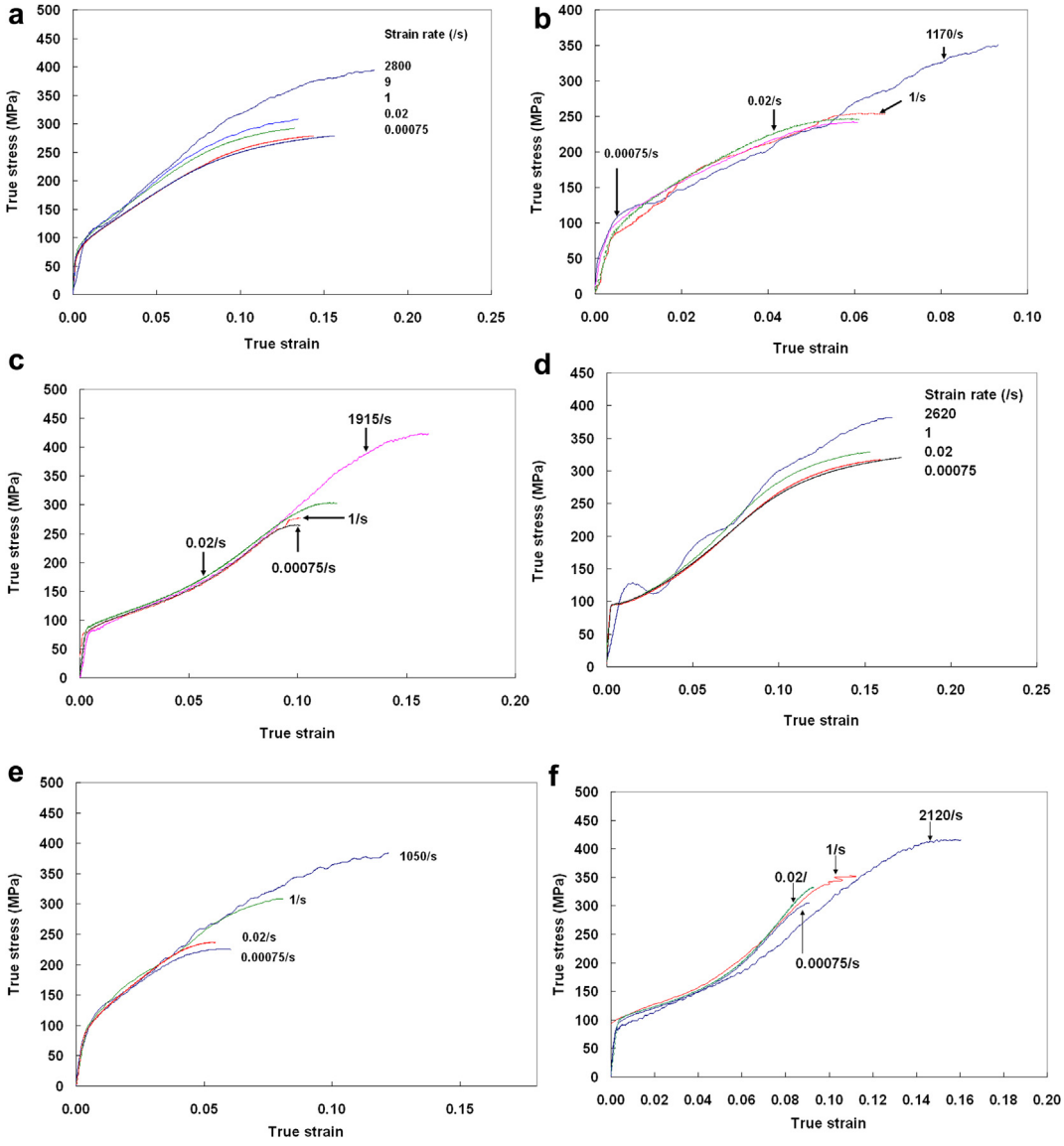

Fig. 7. Effects of strain rate on flow curve of twinning-dominant deformation of the AM30 and AZ31 extrusions. (a) AM30 extrusion, tensile/TD (b) AM30 extrusion, compressive/TD (c) AM30 extrusion, compressive/ED (d) AZ31 extrusion, tensile/TD (e) AZ31 extrusion, compressive/TD (f) AZ31 extrusion, compressive/ED.

Table 4
Orientation, loading, deformation mechanism and sensitivity to thermal effect

Alloy/processing	Specimen orientation	Loading	Deformation mechanism	Sensitivity to rate and temperature
AM30/extrusion	ED	Tensile	Dislocation slip	Moderate
		Compressive	Tension twinning	Negligible
	TD	Tensile	Tension twinning	Negligible
		Compressive	Double twinning	Negligible
AZ31/extrusion	ED	Tensile	Dislocation slip	Moderate
		Compressive	Tension twinning	Negligible
	TD	Tensile	Tension twinning	Negligible
		Compressive	Double twinning	Negligible
AZ31/sheet	RD	Tensile	Dislocation slip	Moderate
	TD	Tensile	Dislocation slip	Moderate
AM50/die casting	–	Tensile	Dislocation slip	Moderate or small
AM60/die casting	–		Dislocation slip	Moderate or small

that the stress–strain curves for slip-dominant deformation are parallel to each other upon changing strain rate and temperature; in other words, that only the thermal component of the flow stress is affected by changes in temperature and strain rate. This is a reasonable approximation based on experimental results (e.g. Refs. [9,11]). The agreement between the constitutive equations and data obtained from the SHB technique is reasonably good (Fig. 6). For HPDC alloys, the stress–strain curves of AM50 and AM60 from the SHB tests showed expected higher yield strength but unexpected lower work-hardening rates than those tested at lower strain rates using the conventional universal test machine. Flow stresses from the SHB tests became lower than those from the universal test machine at strain of 4%–8% for HPDC AM50 and 3%–5% for HPDC AM60, respectively. This reduced work-hardening may result from adiabatic heating.

3.2.2. Twinning-dominant deformation

For twinning-dominant deformation, yield strengths over the strain rate range from quasi-static to 2800 $s^{-1}$are not sensitive to strain rate and temperature owing to the athermal characteristics of mechanical twinning. Stress–strain curves are compared graphically in Fig. 7.

Effects of strain rate and temperature on flow stress may become more pronounced with increasing deformation, i.e. with exhaustion of twinning and increasing proportion of slip. Table 4 summarizes the tests performed in this work, the most likely deformation mechanisms based on texture and metallographic examinations and the sensitivity to strain rate and temperature.

4. Conclusions

Five commercial Mg alloys were tested in uniaxial deformation to determine their flow strength as a function of strain rate, temperature, orientation and loading mode. The following conclusions can be drawn:

1. Non-basal slip-dominant deformation occurs when tension is applied parallel to the basal planes, and was observed for extrusion specimens taken along the extrusion direction (ED) and for sheet specimens loaded in tension along the rolling and transverse directions (RD and TD). High-pressure die castings usually have random textures and fine grains, and the deformation mechanisms of HPDC are slip accommodated by twinning (i.e. primarily-slip-dominant). In primarily-slip-dominant deformation, the true stress–strain curves showed approximately power-law behavior, and the effects of strain rate and temperature on yield strength could be adequately described by constitutive equations linearly dependent on the rate parameter.
2. In primarily-twinning-dominant deformation, which was observed for extrusion specimens loaded in tension in the TD, and in compression in the ED and the TD, the shape of stress–strain curves depends on the twinning type (i.e. twins producing tension strain or double-twins leading to compression strain in the *c*-axis direction). The effects of strain rate and temperature on yield and initial flow stress were small or negligible for strain rates from quasi-static to 2800 s^{-1} owing to the athermal characteristics of mechanical twinning.

Acknowledgments

This work is part of the crashworthiness R&D task of an on-going Canada–China–US Magnesium Front-End Research and Development (MFERD) project. The Canadian task is funded by the CCT&I and ASM-NGV programs, Government of Canada. The leaders of the three-country MFERD projects are gratefully acknowledged for their continuous support, useful discussions and help. Materials were provided by the extrusion, sheet and casting tasks in the MFERD project and the contributions of the personnel involved is gratefully acknowledged.

References

[1] P.G. Partridge, Metall. Rev. 12 (1967) 69–194.
[2] S. Miura, S. Yamamoto, K. Ohkubo, T. Mohri, Mater. Sci. Forum 350–351 (2000) 183–188.
[3] M.R. Barnett, Mater. Sci. Eng. 464A (2007) 1–7.
[4] M.R. Barnett, Mater. Sci. Eng. 464A (2007) 8–16.
[5] A. Jain, S.R. Agnew, Mater. Sci. Eng. 462A (2007) 29–36.

[6] L. Jiang, J.J. Jonas, R.K. Mishra, A.A. Luo, A.K. Sachdev, S. Godet, Acta Mater. 55 (2007) 3899−3910.
[7] M.G. Lee, R.H. Wagoner, J.K. Lee, K. Chung, H.Y. Kim, Int. J. Plast. 24 (2008) 545−582.
[8] A.A. Luo, E. Nyberg, K. Sadayappan, W. Shi, in: M.O. Pekguleryuz, N.R. Neelameggham, R.S. Beals, E.A. Nyberg (Eds.), Magnesium Front End Research and Development: a Canada−China−USA Collaboration. Magnesium Technology 2008, The Minerals, Metals & Materials Society, 2008, pp. 3−10.
[9] S. Xu, W.R. Tyson, R. Bouchard, V.Y. Gertsman, J. Mater. Eng. Perform. 18 (2009) 1091−1101.
[10] S.I. Hill, S. Xu, A.A. Luo, D.A. Wagner, Dynamic Tension and Compression Properties of Extruded AM30 Magnesium Alloy, in: Proceedings of 2009 SEM Annual Conference & Exposition on Experimental and Applied Mechanics, Society for Experimental Mechanics (SEM), Albuquerque, New Mexico, USA, June 1−3, 2009. Paper 450.
[11] S. Xu, W.R. Tyson, R. Bouchard, R. Eagleson, Mater. Sci. Forum 618−619 (2009) 527−532.
[12] S.R. Agnew, in: H.I. Kaplan (Ed.), Plastic Anisotropy of Magnesium Alloy AZ31B Sheet, Magnesium Technology 2002, TMS, 2002, pp. 169−174.
[13] S. Xu, M.A. Gharghouri, M. Sahoo, Adv. Eng. Mater. 9 (2007) 807−812.